Extreme CO_2 concentrations in acidic pit lakes provoked by water/rock interaction

Javier Sánchez-España[¥,*], Bertram Boehrer[§], Iñaki Yusta[β]

[*,¥] Geological Survey of Spain (IGME), c/Calera, 1, 28760, Tres Cantos, Madrid, Spain, [§] Helmholtz Center for Environmental Research – UFZ, Brueckstrasse 3a, D ~ 39114 Magdeburg, Germany, and [β] University of the Basque Country (UPV/EHU), Apdo. 644, Bilbao, Spain.

Supporting Information

Contains 9 figures (S1-S11), two tables (S9 and S12), Extended Methods section (S5) and additional references (S13)

A video file (S7) is provided separately

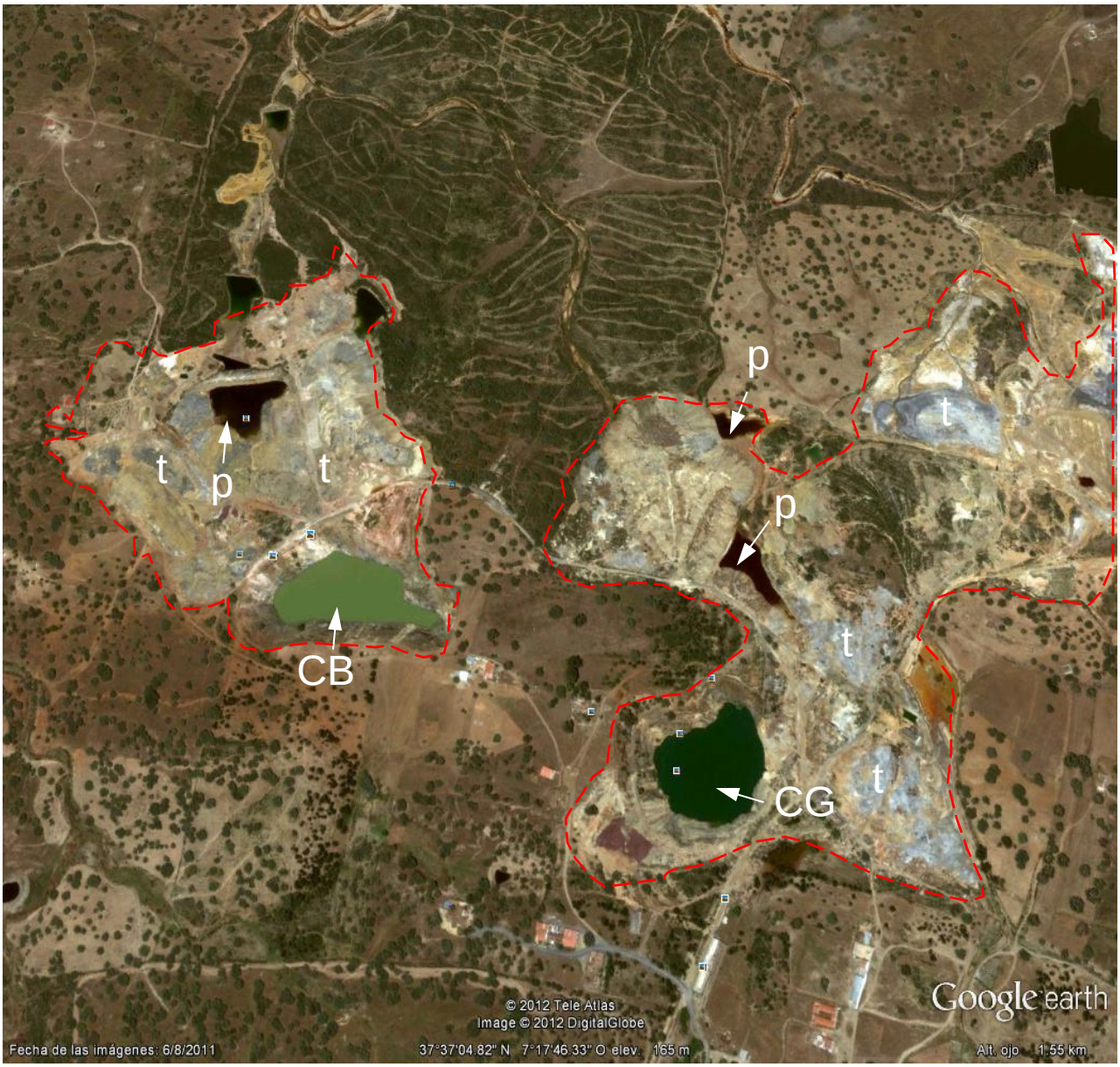

Satellite image of the Herrerías mine site. The red, dashed line approximately encloses the mining works, including the open pits (Corta Guadiana, CG; Corta Santa Bárbara, CB), sulfide-rich tailings (t) and the ponds of acidic mine water (p). Downloaded from Google Earth on 6/8/2011.

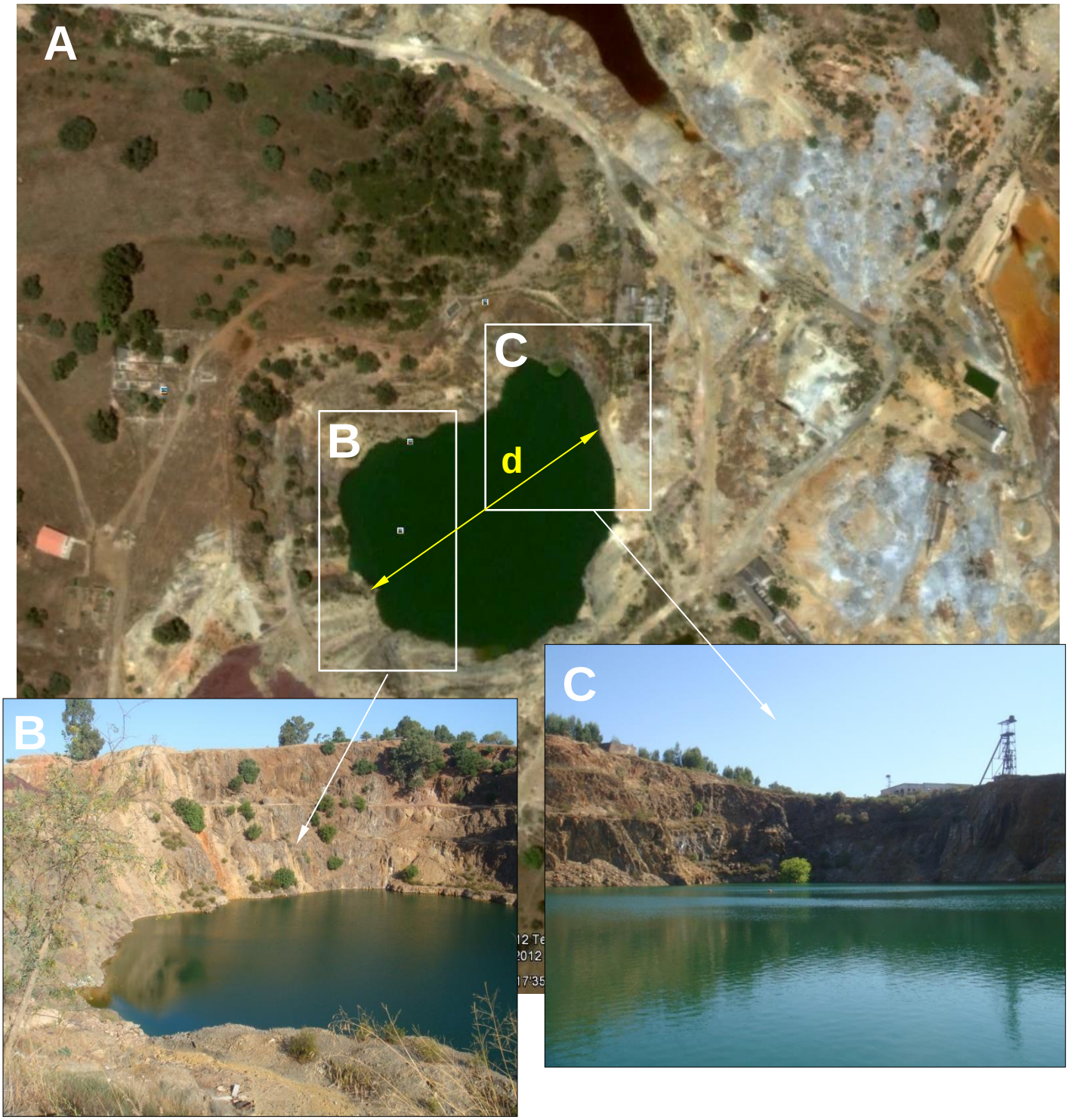

(A) Detail of Figure S1, with insets showing the present-day aspect of the lake formed in Guadiana mine pit: Southwest view **(B)** and Northeast view **(C)**, which includes the old buildings around the former "Guadiana shaft". The yellow line (d) in (A) is 160 m in length. Pictures taken on July 5th, 2011.

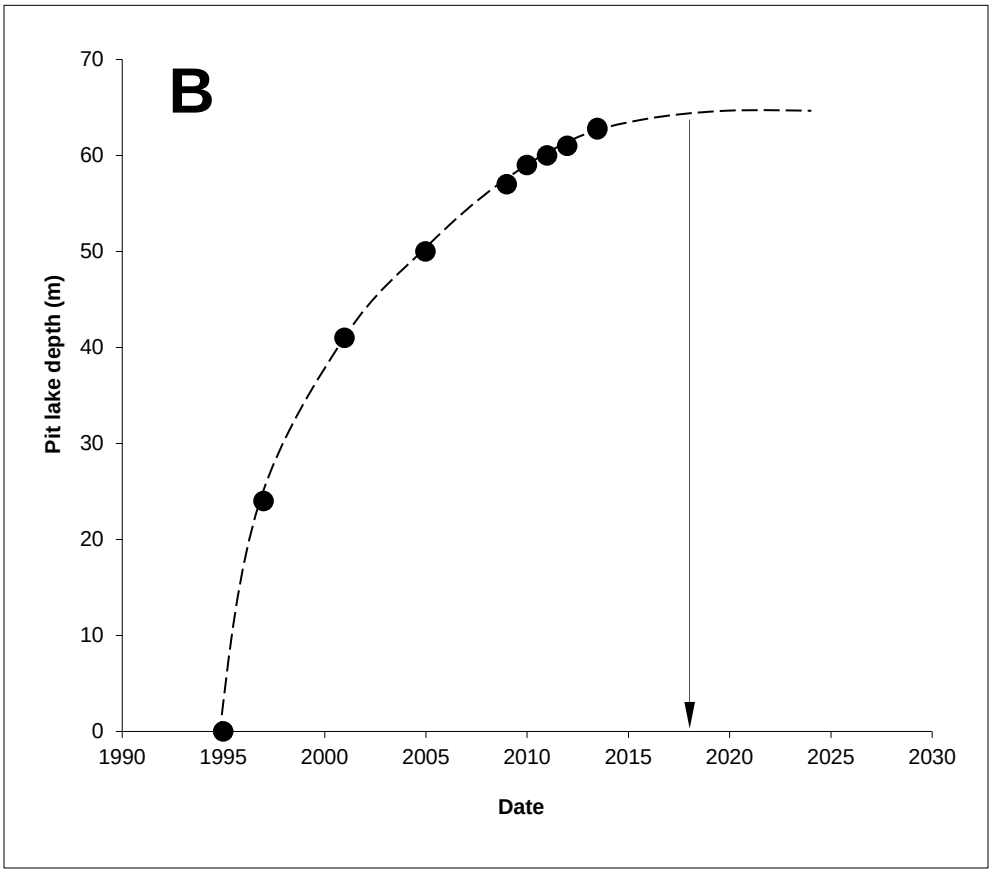

(A) Panoramic view of Guadiana open pit taken in 2005, with indication of the present-day level of the pit lake. **(B)** Evolution of the pit lake depth since 1995 (approximate date for the beginning of the pit flooding) until present. The historical data for 1995, 1997 and 2002 have been deduced from available reports and historical pictures. Extrapolation of the best-fit, regression line gives an approximate date for steady-state conditions by 2018.

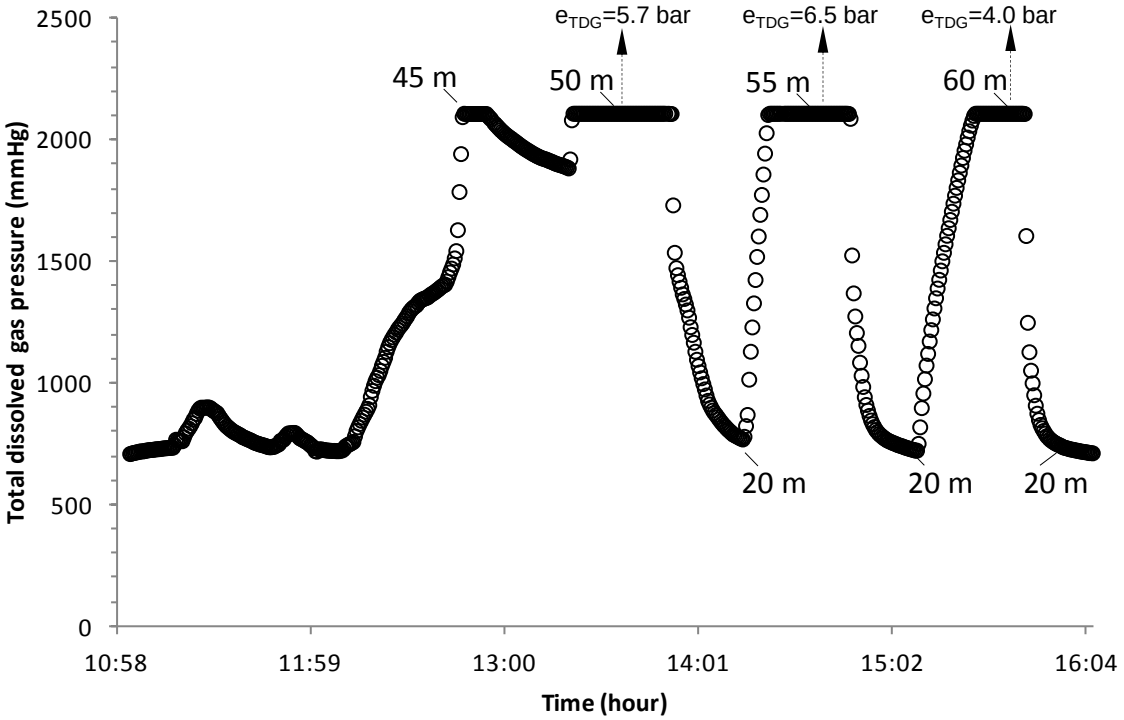

Readings of total dissolved gas pressuse (TDG, in mmHg) *vs*. time obtained in September 2011. The TDG recordings were made with a Hach sensor previously callibrated with atmospheric pressure. The TDG plateaus correspond to the depths at which the sensor was allowed to stabilize for 30 min. The values obtained by extrapolation (e_{TDG}) are indicated for these depths. The valleys with minimum values around 800 mmHg correspond to a depth of 20 m.

S5 - Extended Methods Section

CO_2 partial pressure and concentration. The extrapolation results shown in the previous page (S4) suggested a worrying situation with TDG pressures close to the point of ebullition. Thus, we wanted to avoid dropping the pressure by suction (e.g. successful sampling methods in volcanic lakes; Kusakabe 2000). Consequently, a small pump was dropped on its cable to the required depth. A gas-tight sampling bag (3 l volume, Tesseraux, Germany) was attached through a holding valve. A CTD probe recorded depth (i.e. pressure), temperature and conductivity, while the pump was switched on for about 3 s to fill 0.4 l of lake water into the bag. Then the sampling bag was recovered and safely closed. Samples were taken from depths of 0.1, 20, 35, 40, 45, 50 and 55 m. Under the water pressure of 60 m, the pump failed.

The sampling bags were taken to the field accommodation and the weight was measured on a weight scale (the weight of the empty bag had been previously measured). Then the bags were placed in an air-conditioned room of 18.8°C, while from time to time ebullition and redissolution were supported by carefully shaking the bags. After a few hours, the bags contained both a water phase and a gas phase at atmospheric pressure. The volumes of the bags were determined by submerging them in a water-filled container. After removing the sampling bag the container was put on a weight scale to quantify the missing water mass, and hence retrieve the volume of the gas bubble after subtracting the volume of the water (mass and density was known) and the volume of the empty bag (measured before). Considering the different sources of error, the accuracy of this technique has been estimated in around ca. ±0.030 ml. The gas volume in the deeper samples could be measured within 5 to 20 % relative error. Other errors, temperature and salinity-dependent Bunsen coefficients (Murray and Riley, 1971) lay in the range of 5%. Thus, we could present reliable measurements of CO_2 concentrations up to depths to 55 m. The results of gas volume and CO_2 partial pressure are shown in the following table. The resulting CO_2 concentrations deduced are given in Table 1.

Gas volume and CO_2 partial pressure measured in the Guadiana pit lake on December 2013.

Depth *(m)*	***Gas volume*** *(L)*	***CO_2 partial pressure*** *(bar)*
0	*0.0217*	--
20	*0.0117*	--
35	*0.1707*	*1.6706*
40	*0.2107*	*1.7077*
45	*0.2677*	*2.2664*
50	*0.6887*	*3.5522*
55	*0.5307*	*3.6025*

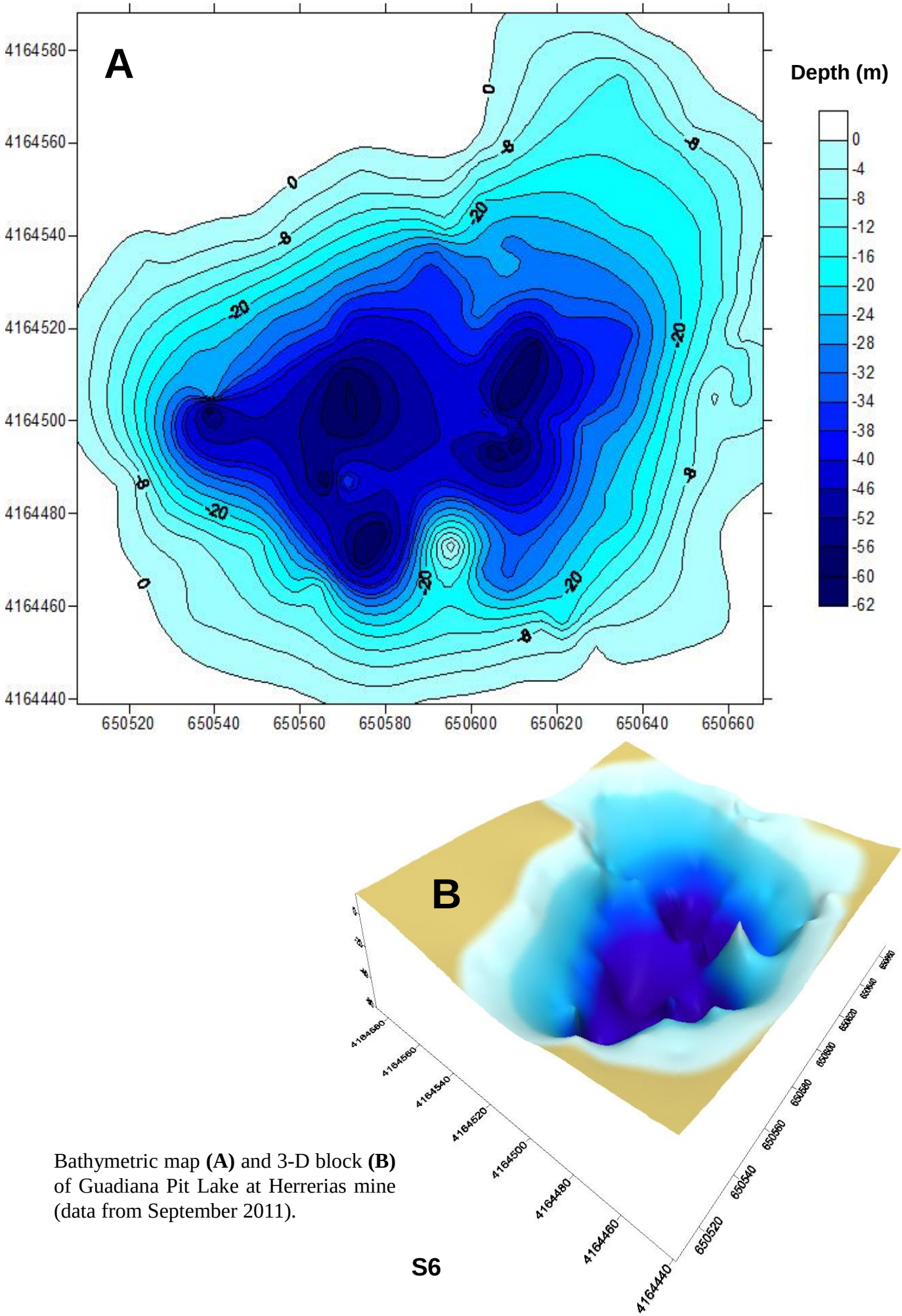

Bathymetric map **(A)** and 3-D block **(B)** of Guadiana Pit Lake at Herrerias mine (data from September 2011).

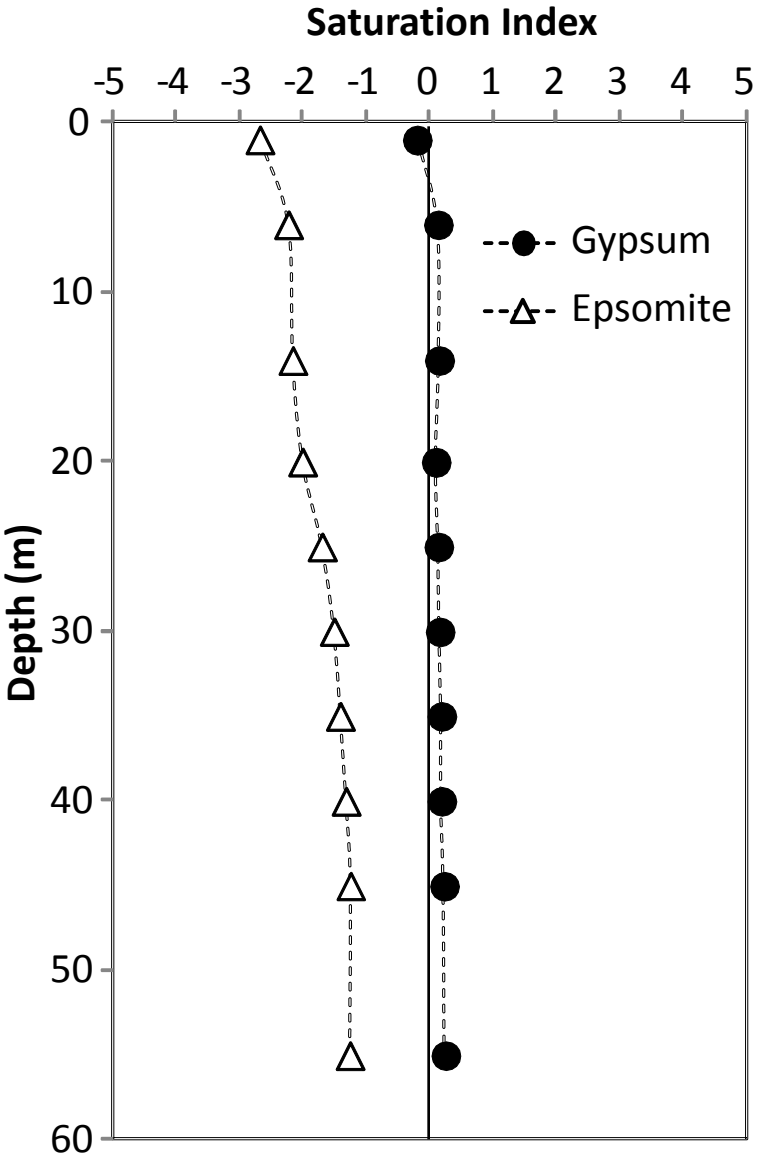

Vertical profiles of gypsum ($CaSO_4 \cdot 2H_2O$) and epsomite ($MgSO_4 \cdot 7H_2O$) saturation indices (where SI=[log IAP/Log K_{sp}])) in the Guadiana pit lake at Herrerías mine. The calculated SI values correspond to the water chemistry observed in September 2011.

Selected results of neutralization experiments with different rocks from the IPB

					Composition of final solution (*mg/L*)									
Rock type	**Mineralogy (XRD)**	**%CO_3^{2-} (1)**	**pH_o**	**pH_f**	**SiO_2**	**SO_4**	**Na**	**K**	**Mg**	**Ca**	**Al**	**Fe**	**HCO_3^-**	**CO_2(2)**
Sedimentary rocks														
Gray shale	Qtz, Mc, Chl, K-Fd	<1	2,00	3,90	55	14	8	5	85	28	9,3	0,01	*n.a.*	30
Gray shale	Qtz, Mc, Chl, K-Fd		1,60	3,28	62	95	7	5	86	66	*n.a.*	*n.a.*	17	73
Green shale	Qtz, Mc, Chl, K-Fd		1,60	3,60	48	11	27	7	56	40	*n.a.*	*n.a.*	18	44
Purple shale	Qtz, Mc, Chl, K-Fd, Hem, Ca	2-3	2,00	4,38	25	<10	3	2	27	153	1,1	0,02	*n.a.*	168
Volcanic rocks (IPB)														
Rhyolite	Chl, Qtz, Pla, Mc, Ca, Py	4-5	2,00	8,46	14	530	14	3	29	391	0,4	0,05	*n.a.*	430
Rhyolite	Chl, Qtz, Pla, K-Fd, Mc, Ca		1,90	7,20	9	44	12	3	26	98	*n.a.*	*n.a.*	35	108
Riodacite			1,90	3,50	43	22	4	14	28	85	*n.a.*	*n.a.*	14	94
Basic volcanic			1,90	7,66	9	16	5	3	23	168	*n.a.*	*n.a.*	56	185
Basic volcanic			1,60	7,50	6	32	5	16	14	126	*n.a.*	*n.a.*	59	139
Volcanic rocks (Herrerías)														
Spilite	Pla, Chl, Px, Ca (Qtz)	18	1,50	7,20	18	*n.a.*	10	41	78	910	*n.a.*	*n.a.*	*450*	1110
Spilite	Pla, Chl, Ca (Px, K-Fd)	12	1,50	6,80	21	*n.a.*	9	12	56	1032	*n.a.*	*n.a.*	460	1260
Spilite	Pla, Chl, Px, Ca (Qtz)	24	1,50	7,70	25	*n.a.*	10	5	69	1040	*n.a.*	*n.a.*	550	1270
Sulphide mineralization														
Pyrite ore	Py, Cpy, Sd, Ca	6-8	6,00	3,60	8	6200	6	1	37	545	6,5	2883	*n.a.*	600

Abbreviations: Qtz, quartz; Chl, chlorite; Mc, illite/muscovite, K-Fd, potassic feldspar; Pla, plagioclase; Hem, hematite; Ca, calcite; Py, pyrite; Cpy, chalcopyrite; Sd, siderite; Px, piroxene; pH_o, initial pH of acidic solution; pH_f, final pH of neutralized solution (after 60 days); n.a., not analyzed.

(1) Estimated by XRF and optical examination of thin sections.
(2) Carbon dioxide theoretically released by calcite dissolution (calculation based on Ca concentration)
(3) for pH=8,5, most of the initially released CO_2 should be actually present as HCO_3^- and CO_3^{2-}.

Neutralization experiments. For the acid neutralization experiments, crushed rock fragments were placed in plastic containers (1 liter volume), filled with Milli-Q water previously acidified to pH 1.5-2.0 with concentrated H_2SO_4 and/or HCl, and stored at ambient conditions (25ºC) for 30-60 days. Similar time and environmental conditions were followed for the pyrite dissolution experiments, where crushed fragments of massive sulfide mineralization (containing dominant pyrite, minor chalcopyrite and trace gangue minerals) were submersed in pH 6.0 sterile solution (1 L). In all cases, a small air space was left in the top of the containers, which were also subject to sporadic shaking. The water/rock volume ratio was approximately 1:4. The solution pH was continuously monitored with a hand pH meter. At the end of the experiments, the waters were 0.45 μm-filtered, and the final composition of the solutions was analyzed by AAS (Na, K, Mg, Ca, Al, Fe), ICP-AES (S, given as SO_4^{2-}; Si, given as SiO_2) and ionic chromatography (HCO_3^-).

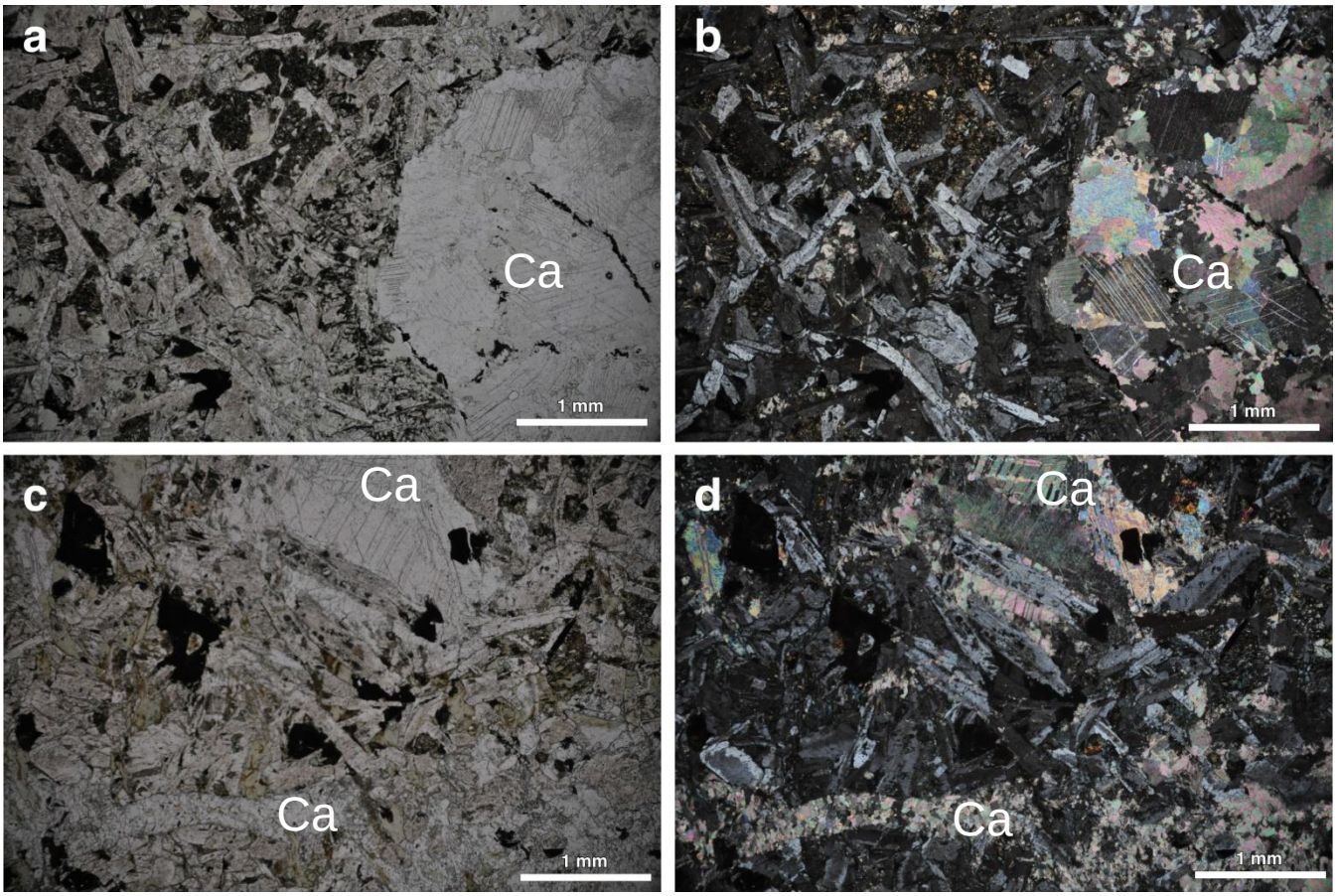

Photomicrographs of spilitic rocks from Herrerías mine
(obtained in thin sections by transmitted light optical microscopy, TLOM)

Spilite rocks from Herrerías mine show different textural types of calcite. Calcite (Ca) can be found filling vacuoles (a, b) and microveins (c, d), but also also as dispersed cement in the groundmass with grain sizes ranging from 0.05 mm up to 1 mm in twinned crystals. In addition to calcite, these spilitic rocks are mainly composed by sodic plagioclase laths, partially chloritized pyroxene, and minor quartz and titanite. Chlorite is recognized replacing mafic crystals and in the groundmass. Transmitted light photomicrographs taken in plane-polarised (PPL, a and c) and cross-polarized light (XPL, b and d).

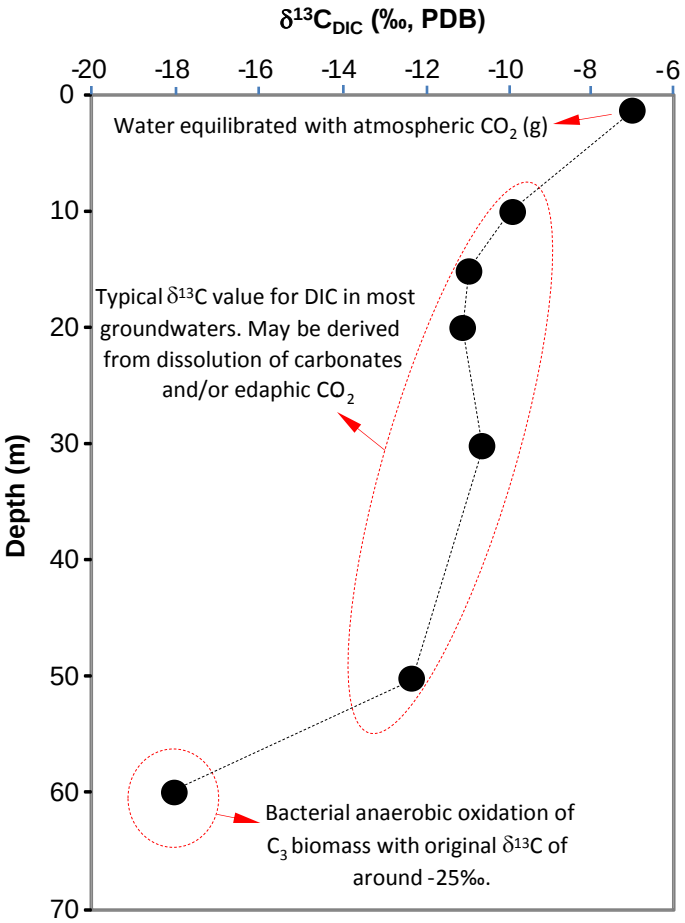

Isotopic composition of dissolved inorganic carbon ($\delta^{13}C_{DIC}$) in the Guadiana pit lake; the most probable C sources are indicated.

Compilation of $\delta^{13}C$ signatures of diverse carbon pools near Herrerías mine

Sample description	$\delta^{13}C_{PDB}$ (‰)	Reference
Dissolved inorganic carbon in local creeks [(1)]		
Rivera del Huelva	-13,5	*This study*
Rivera Olivargas	-12,1	*This study*
Arroyo Tamujoso	-14,6	*This study*
Rivera Escalada	-10,2	*This study*
Bco. Juliana	-13,1	*This study*
Average	***-12,7***	
Organic matter from plants and wood in the area		
Wood from mine shaft	-24,3	*This study*
Heather	-26,3	*This study*
Oleander	-26,2	*This study*
Gluy bush	-30,6	*This study*
Pine needles	-26,0	*This study*
Broom (Ginster)	-27,3	*This study*
Pine cone	-27,4	*This study*
Mimosa-like bush	-29,3	*This study*
Wood from door case	-26,1	*This study*
Eucalyptus	-28,1	*This study*
Average	***-27,2***	
Carbonates in Guadiana pit (Herrerías mine) [(2)]		
Mg-Calcite in spillitic lava	-14,2	*This study*
Mg-Calcite in spillitic lava	-14,9	*This study*
Mg-Calcite in spillitic lava	-14,7	*This study*
Hydrothermal carbonates in other sulphide mineralizations		
Ankerite (*Aguas Teñidas)*	*-4,1*	*[1]*
Ankerite (*Aguas Teñidas)*	*-4,7*	*[1]*
Ankerite (*Aguas Teñidas)*	*-7,6*	*[1]*
Ankerite (*Aguas Teñidas)*	*-7,6*	*[1]*
Ankerite vesicle in spilite (*Tharsis)*	*-10,1*	*[2]*
Ankerite (*Tharsis)*	*-9,3*	*[2]*
Ankerite vein is spilites (*Tharsis)*	*-9,2*	*[2]*
Siderite ore (*Tharsis)*	*-9,7*	*[2]*
Siderite ore (*Tharsis)*	*-6,4*	*[2]*
Siderite (*Masa Valverde)*	*-9,5*	*[3]*
Siderite (*Masa Valverde)*	*-3,1*	*[3]*
Average	***-7,4***	

(1) Near-neutral, pristine waters with dissolved inorganic carbon mainly as HCO_3^-.

(2) $\delta^{13}C$ data obtained by dissolution of calcite during neutralization experiments with volcanic rock fragments and subsequent analyses of HCO_3^- in the final solutions. The chemical composition and mineralogical features of these rocks are shown in pages S9 and S10 of this supporting information. The results of the experiments are provided in Figure 6b.

References: [1] Sánchez-España, 2000; [2] Tornos et al., 1998; [3] Toscano et al., 2000.

References (Supporting Information)

Kusakabe, M., Tanyileke, G.Z., McCord, S.A., Schladow, S.G. Recent pH and CO_2 profiles at Lakes Nyos and Monoun, Cameroon: implications for the degassing strategy and its numerical simulation. *J. Volcano. Geotherm. Res.* **2000**, 97 (1-4), 241-260.

Murray, C. Riley, J. The solubility of gases in distilled water and sea water—IV. Carbon dioxide. *Deep Sea Research and Oceanographic Abstracts* **1971**, 18-5, 533-541.

Nelson, S.T. A simple, practical methodology for routine VSMOW/SLAP normalization of water samples analyzed by continuous flow methods. *Rapid Communications in Mass Spectrometry* **2000**, 14, 1044-1046.

Sánchez-España, J. Mineralogy and geochemistry of massive sulphide deposits in the Northern Iberian Pyrite Belt (San Telmo-San Miguel-Peña del Hierro), Norte de Huelva, España. Ph.D. Thesis Dissertation, University of the Basque Country, Bilbao, 2000, 307 p. (plus apendix).

Tornos, F., González Clavijo, E., Spiro, B. The Filón Norte orebody (Tharsis, Iberian Pyrite Belt): a proximal low-temperature shale-hosted massive sulphide in a thin-skinned tectonic belt. *Mineralium Deposita* **1998**, 33, 150-169.

Toscano, M., Sáez, R., Almodóvar, G.R. Carbonatos hidrotermales asociados al depósito de sulfuros masivos “Masa Valverde” (Faja Pirítica Ibérica): Características texturales y geoquímicas. *Cadernos Lab. Xeolóxico de Laxe* **2000**, 25, 423-425